32nd EPS Conference on Plasma Phys. Tarragona, 27 June - 1 July 2005 ECA Vol.**29C**, P-2.056 (2005)

Relaxed State of Reversed Field Pinch Equilibrium with Low Aspect Ratio

S. Shiina[1], Y. Nagamine[2], M. Taguchi[3], Y. Osanai[2], Y. Kondoh[4], K. Kusano[5], Y. Yagi[1], H. Sugimoto[1], H. Ashida[1], K. Saito[2], M. Aizawa[2], M. Watanabe[2], H. Koguchi[1], Y. Hirano[1], H. Sakakita[1]

[1] *National Institute of Advanced Industrial Science and Technology, Tsukuba, Japan*

[2] *Institute of Quantum Science, Nihon University, Chiyoda-ku, Tokyo, Japan*

[3] *College of Industrial Technology, Nihon University, Narashino, Japan*

[4] *Departmentf Electronic Engineering, Gunma University, Kiryu, Gunma, Japan*

[5] *Department of Material Science, Factory of Science, Hiroshima University, Hiroshima, Japan*

1. Introduction. Woltjer and Taylor have concluded that a small-scale turbulence causes a plasma to relax to equilibrium with a relative minimum of the energy integral E, and then the turbulence decays [1]. The minimization occurs because the dissipation of energy is rapid in comparison with that of the helicity in the case of a short-wave turbulence. As a result, the relative energy minimum becomes an attractor. In the course of this relaxation, however, the plasma pressure p vanishes since there are no limitations on a minimum in term of p. In this report, the finite beta effects on the plasma relaxation are considered for two types of reversed field pinch (RFP), the partially relaxed state model (PRSM) and the neoclassical equilibrium solved self-consistently considering the self-induced plasma current.

2. Partially relaxed state model (PRSM). As one of the finite beta RFP configuration reasonably close to a stable minimum energy state, the relaxed state if a nonideal MHD plasma is considered. The energy principle of a nonideal MHD plasma with the losses of mass M, entropy S and helicity K leads to the sufficient condition for the relaxed states with minimum energy [2]. Recently, both the generalized vortex flux and the self-helicity have been shown not to be invariant in an ideal to fluid plasma as well as the prediction based on energy principle of a non-ideal MHD plasma. The stationary state and the stability are formulated as $\delta F = 0$ and $\delta^2 F > 0$, respectively where F is the free energy function defined by $F = W - \lambda_0 K - \kappa_0 M - T_0 S$; δF and $\delta^2 F$ are the first and second variations of F; W is the potential energy to be minimized in the energy principle, λ_0, κ_0 and T_0 are the Lagrange multipliers, respectively. Using the variational technique, the Euler-Lagrange equation for arbitrary vector potential variations of δA, which is obtained from the volume integral term of $\delta F = 0$ when the ideally conducting wall at plasma boundary is assumed, gives an equilibrium equation in the orthogonal magnetic coordinate system (ψ, θ, ϕ),

$$\boldsymbol{j} = \lambda \boldsymbol{B} / \mu_0 + (\mathrm{d}p / \mathrm{d}\psi)(\nabla\phi / |\nabla\phi|^2) \qquad (1)$$

where λ and p have their own unique profiles with respect to ψ as $\lambda = \lambda_0 g(\psi)$ and $p = p_0 p(\psi)$, respectively. Here, ψ is the poloidal flux outside each magnetic surface, θ and ϕ are the coordinates in the poloidal and the toroidal direction, respectively, and $\boldsymbol{B}$ is given as $\boldsymbol{B} = \nabla\psi \times \nabla\phi + RB_\phi \nabla\phi$ (R is distance from symmetrical axis). The stationary state of eq. (1) has the force-free magnetic fields for poloidal direction, $(\nabla \times \boldsymbol{B})_\theta = \lambda(\psi)\boldsymbol{B}_\theta$, so called partially relaxed state model (PRSM) condition, and is generally equivalent to the Grad-Shafranov equation for the axis symmetric toroidal equilibria with $\mathrm{d}I(\psi) / \mathrm{d}(\psi) = \lambda(\psi)/\mu_0$, where $I(\psi)$ means the current flux function. Again using the variational technique, the sufficient condition for the minimum-energy state is obtained from $\delta^2 F > 0$.

The features of relaxed state with minimum energy at finite beta for the PRSM-RFP equilibrium is supported by the MHD simulation for the relaxation process in RFPs [3, 4]. The relaxed state dynamically achieved by the simulation has a flat pressure profile well approximated by Bessel function model in the central region. As shown in Fig. 1, the profile of $j_\theta / B_\theta (\equiv \lambda / \mu_0)$ in the relaxed state is almost uniform over the wide region, and in the central region the profile of j_z / B_z also has the same one as j_θ / B_θ. But in the outer region the j_z / B_z profile is far deviated from a constant value and ultimately becomes negative near the wall. These profiles are consistent with predictions by the PRSM-RFP in the case of λ = constant except the plasma periphery. Also, the profile of the ratio of scalar product $\boldsymbol{j} \cdot \boldsymbol{B}$ to $\boldsymbol{B} \cdot \boldsymbol{B}$ is shown to be nearly same as the λ-profile, which is consistent with that in the PRSM-RFPs with constant λ, namely, $\boldsymbol{j} \cdot \boldsymbol{B} / B^2 = \lambda / \mu_0 - (B_z / B_\theta B^2)(\mathrm{d}p / \mathrm{d}r)$. The PRSM-RFP has the stability property that the internal tearing modes are found to be stable having a rather higher stability β limit than that for the ideal kink modes in the cylindrical PRSM plasma being compressible with a magnetic Reynold number of 3.0×10^3, a normalized viscosity coefficient of 3.3×10^{-4} and a thermal conducting coefficient of 1.0×10^{-4} [4]. Finally the resistive interchange (*g*) mode instability should be examined considering the neoclassical effects such as viscosity, magnetic shear and favorable magnetic line of force curvature, which play important roles in low-*A* configuration.

Fig. 2 shows the comparison of $\boldsymbol{j}\cdot\boldsymbol{B}/B^2$-profile without and with rf- driven current when the plasma β at the center is 10%. The initial state is given by an unstable force-free state which 8.7% higher energy compared with the Taylor's minimum energy state. It shows the time history of $\boldsymbol{j}\cdot\boldsymbol{B}/B^2$-profile for the injected rf power of P_0 = 0, 2 and 4 [MW]. For P_0 = 0 (without rf injection), the strong MHD relaxation takes place t = 670 Alfven transit time, and the λ-profile on the central region is quickly flattened. It means that the toroidal current in the central region is converted to the poloidal current in the outer region. For P_0 = 2 [MW], the weak MHD relaxation is observed, and for P_0 = 4 [MW], the relaxation- free process is achieved. Fig. 3 denotes the relationship between the time averaged magnetic energy of the kink mode (m = 1) and the injected high power rf power.

It is also observed that the field reversal ratio decreases below zero as P_0 increases, and the quiet sustainment of the reversed field is realized when the rf power is injected into the plasma. However, the PRSM condition of uniform j_θ / B_θ-profile is not satisfied in the neoclassical RFP equilibrium, as shown in Fig. 4. But the magnetic shear is larger than that in the classical (PRSM) equilibrium, where the Robinson's stability criterion (cylindrical approximation) against ideal kink mode is satisfied for any plasma pressure profiles in present study, the stability beta limit is determined by Mercier's mode rather than the ideal kink mode.

In order to find out a dynamo-free, neoclassical RFP configuration and improve the energy confinement time, the features of minimum energy state for the neoclassical RFP equilibrium is examined taking into account of Lyapunov functional model as follows.

3. The Lyapunov functional model. The Lyapunov functional model which is proposed as a condition for a minimum of energy *E* and pressure *p*, again uses the energy relaxation principle at a given constraint [5, 6]. This constraint is obtained in the frame of the usual set of MHD equations, but compared with total magnetic helicity *K* = const. it looks like a more general one: $M = \int h\mathrm{f}\,(p^{1/\gamma} / h)\, d^3x$ = const., which contains the pressure *p*. Here γ is the adiabatic index of the plasma and f is an arbitrary function. When $p \rightarrow 0$ the function f(0) = const. and *M* is proportional to *K*. Under this more restrictive condition the plasma can relax to a state in which *p* has a significant maximum at the center of the plasma. In other words, a turbulent relaxation realizes a minimum of the Lyapunov functional $L = E + M$, $E = \int[\rho v^2 / 2 + p/(\gamma - 1) + B^2/ 2\mu_0]\, d^3x$, where ρ is the density, and *v* is the plasma velocity. These integrals *E* and *M* where were chosen because they are smooth with respect to the arguments *A*, *p*, *v*, and ρ, so the first and second variations of *L* are also smooth functionals. In the case of a short-wave turbulence, the quantities v^2 and *p* relax most rapidly, because they are sensitive to the turbulent viscosity and to the thermal conductivity. The quantity $B^2 = (\nabla\times\boldsymbol{A})^2$ relaxes more rapidly than $h = \boldsymbol{A}\cdot\boldsymbol{B}$, which satisfies a continuity equation and which contains smaller derivatives. The ratio of the amplitudes of the corresponding fluctuations of these quantities is thus larger that a / λ, where *a* is a length scale of the plasma, and λ is a length scale of the turbulent fluctuations. As a result, if the plasma is in quasi-steady state near a minimum of *L*, a comparatively rapid decrease in v^2, *p* and B^2 sends the plasma into a state with a minimum of *L*, while there is almost no change in *h*. At the *L* minimum the plasma becomes more stable, and the turbulence level should decrease. The extremum $\delta L = 0$ leads to the relaxed-equilibrium equation:

$$\nabla\times\boldsymbol{B} = -\,2H\boldsymbol{B} - \nabla H\times\boldsymbol{A};\ H = H(h);\ \boldsymbol{B} = \nabla\times\boldsymbol{A}. \qquad (1)$$

Here *H*(*h*) is the function of *h* related to the f-function and gives the steady-state pressure as a function of the helicity *h*,

$$p(h) = \int h(\partial H / \partial h)\, dh / \mu_0 + \mathrm{const.} \qquad (2)$$

System of equations (1), (2) singles out a very limited subset of the set of plasma equilibria. In the case of *H* = const., the current is parallel to ***B*** according to eq. (1), and there is a force-free state. The corresponding equation has been solved analytically by Taylor. We find other solutions of eq. (1) numerically in a cylindrical geometry with coordinate system (r, θ, z). For this purpose we assume that all quantities depend on the cylindrical radius r alone. At $r = 0$, we set

$$A_z = \Psi,\quad A_\theta = 0,\quad B_z = 1,\quad B_\theta = 0,\quad (\nabla\times\boldsymbol{B})_z = 1,\quad H = -1/2. \qquad (3)$$

Here Ψ is a constant which, along H, determines the structure of the equilibrium. Conditions (3) introduce units of magnetic field and length, B_z and $B_z / (\nabla\times\boldsymbol{B})_z$, at the magnetic axis. It is convenient to replace $H(h)$ by a function of r; $H = g(r) / 2$. Equation (2) then becomes

$$p(r) = \int_a^r h(\partial g / \partial r)\, dr / 2\mu_0. \qquad (4)$$

By specifying values of g and Ψ, we can find solutions of eq. (1) in the form of axisymmetric configurations. It is interesting to note that eq. (1) gives the possibility to find finite solutions with zero current density near the plasma wall. Solutions of eq. (1) in the form of a reversed field pinch have been reported to have a high current density at the boundary [5].

Let us consider the solution of eq. (1) in the form of the low-aspect-ratio neoclassical RFP equilibrium. For this purpose, we assume that the plasma pressure has a relatively broad profile with the form of $p = p_0 [1 - (r / a)^6]$ in cylindrical geometry approximation. At the axis we have $q_0 \sim 1$, and $h = \Psi$ (< 0) according to eq. (3). The ratio of the pressure to the magnetic pressure at the axis is $\beta_0 = 0.84$, which is related to Ψ by

$$\beta_0 = \int_a^0 h(\partial g / \partial r)dr = -\Psi - \int_a^0 (\partial h / \partial r) g dr$$

according to eq. (4) and increases with decreasing Ψ. The constant value of Ψ, which gives the helicity h at the axis, is determined in conjunction with β_0 by the profiles of $h(r)$ and $g(r)$ in the neoclassical equilibrium. The parallel current and the perpendicular current in the neoclassical equilibrium correspond to the first term (force-free current) and the second term (perpendicular current) considering the neoclassical toroidal effects in eq. (1), respectively. The second term leads mainly to the high current density at the boundary, where the contribution from the first term is negligibly small because of a weak toroidal field there. The toroidal current density at the boundary ($r = a$) is given by

$$j_z \sim [(\partial g / \partial r) A_\theta]_{r=a} / 2\mu_0,$$
$$(\partial g / \partial r)|_{r=a} = -2\mu_0 [(\partial p / \partial r) / h]_{r=a},\ (A_\theta / h)_{r=a} \sim 1$$
$$\sim 3\beta_0 / \mu_0,\ \beta_0 = 2\mu_0 p_0 / B_z^2(0)\ (= 0.84)$$

using eq. (1) and eq. (4). The first term of eq. (1) in a cylindrical geometry gives the j_z maximum of $1/\mu_0$ at the axis and the minimum at the boundary, on the other hand, the second term gives the minimum of $j_z = 0$ at the axis and the maximum of $j_z = 3\beta_0 / \mu_0$ at the boundary, indicating the hollow j_z-profile with the ratio of $j_z(a) / j_z(0) = 3\beta_0$. The broader the pressure is near the axis, the larger the gradient $\partial g / \partial r|_{r=a}$ becomes, the j_z thus is the larger at the boundary. It can be seen from eq. (4) that the $(\partial g / \partial r)$-profile has a larger spatial variation compared to the $(\partial p / \partial r)$-profile since the helicity h increases as the boundary is approached in the RFP.

4.Conclusion. The relaxed-equilibrium equation leads to a hollow profile of toroidal current density higher by factor $3\beta_0$ at the plasma boundary than at the axis, thus is satisfied for the neoclassical RFP equilibrium with a broad plasma pressure profile as shown in Fig.5. Considering the force-free current due to the increasing neoclassical effects with lowering aspect ratio in the relaxed-equilibrium equation, the current profile becomes more hollow in the relaxed- equilibrium state, indicating that the neoclassical RFP equilibrium is close to the relaxed- equilibrium state with a minimum energy.

In discussion the high current density at the boundary is not altogether convenient for fusion purposes, but the presence of bulk bootstrap current flowing near the boundary would help an external control to sustain the high current density at the boundary if necessary because the plasma reversal is not essentially affected by the increasing resistivity near the wall, hence the steady state neoclassical RFP configuration having a broad pressure profile and a hollow current profile can be hold with a dominant plasma self-induced current. It has been proposed to sustain and / or drive the current near the boundary to strengthen the magnetic shear there along the aim to weaken the dependence of stability on conducting wall. The relaxed-equilibrium state can be achieved also by peaking plasma pressure profile with the zero current density at the plasma boundary although the beta value becomes low.

[1] J. B. TAYLOR, Phys. Rev. Lett. **33**, 1139 (1974). [2] K. KONDOH, J. Phys. Soc. Jpn. **58**, 489 (1989). [3] K. KUSANO, J. Phys. SOC. Jpn. **56,** 963 (1987). [4] T. NAGAI, et al., Proc. 8th ICPP (Nagoya, 1996) Vol. 1. P.1042. [5] V. I. PETVIASHVILI, JETP Lett. **57**, 103 (1993). [6] V. A. GOLDIN and V. I. PETVIASHVILI, JETP. **68** (1989) 988.

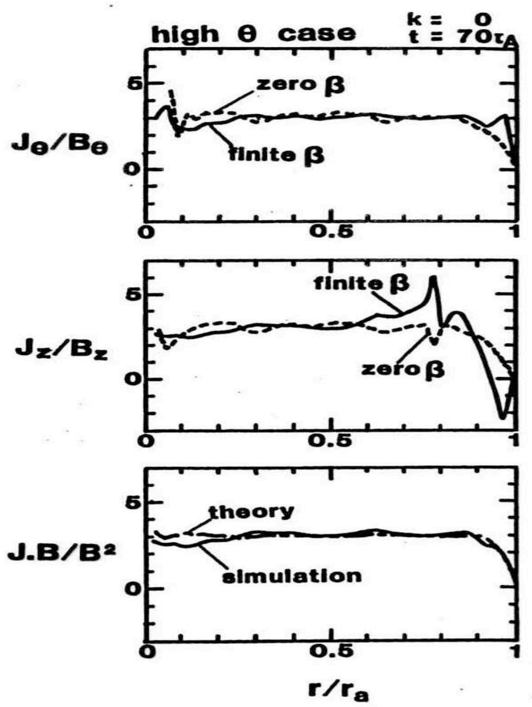

Fig. 1 The radial profile of the ratio J_θ / B_θ, J_z / B_z and $\boldsymbol{J} \cdot \boldsymbol{B} / B^2$ for zero β (dotted line) and finite β (solid line) simulations. The dot-dashed line is the predicted line by partially relaxed state model.

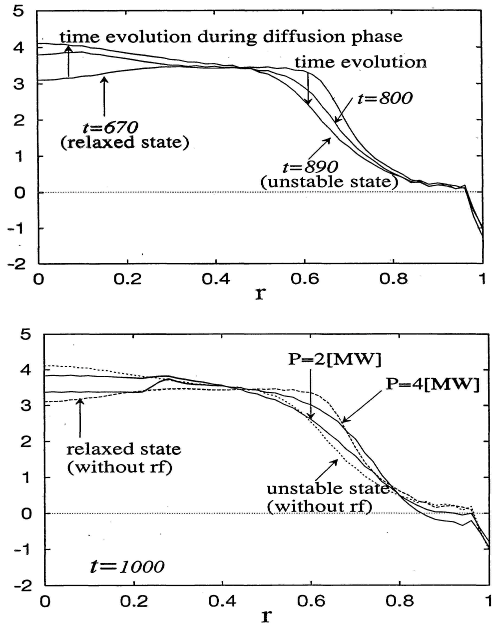

Fig. 2 The upper shows the time evolution of $\boldsymbol{J} \cdot \boldsymbol{B} / B^2$-profile during diffusion phase without rf-driven current, and the lower shows the comparison of $\boldsymbol{J} \cdot \boldsymbol{B} / B^2$-profiles between in the relaxed state without rf-driven current and in the stationary state with rf-driven current.

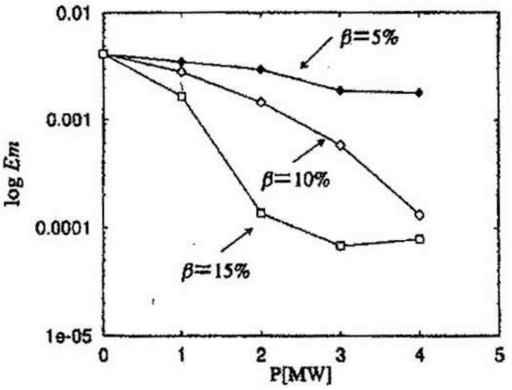

Fig. 3 Kink mode damping as function of rf power for each β value.

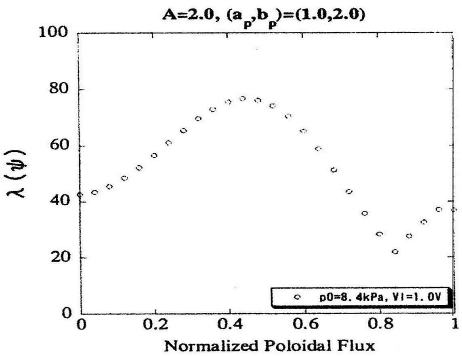

Fig. 4 λ-profile as function of normalized poloidal flux in the neoclassical RFP equilibrium.

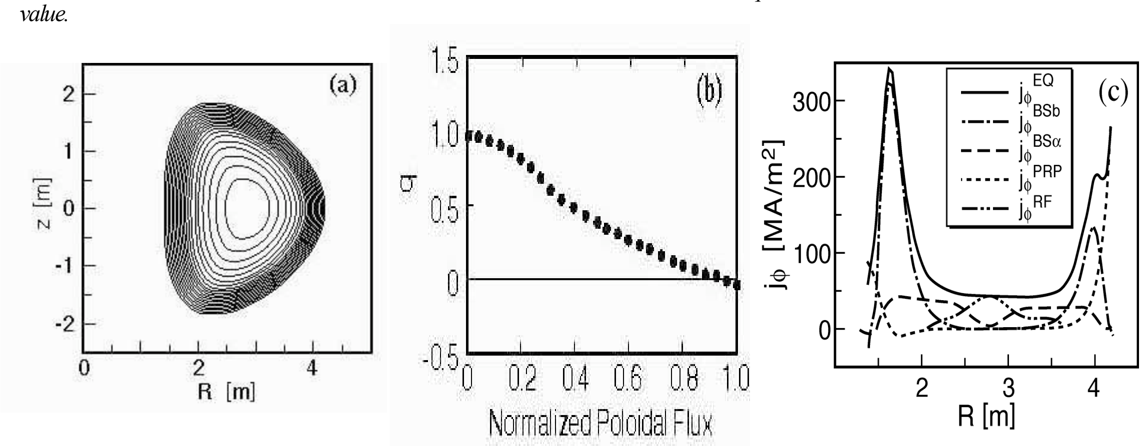

Fig.5 Steady-state neoclassical RFP equilibrium. Magnetic flux surface (a), profile of safety factor q as a function of normalized poloidal flux (b), and profiles of toroidal current density in midplane (c). Note that the equilibrium current j_ϕ^{EQ} has a hollow profile mainly due to the bulk bootstrap current j_ϕ^{BSb}; $j_\phi^{BS\alpha}$ is the bootstrap current due to fusion-produced alpha particle, without considering the finite banana-width effect, j_ϕ^{PRP} is the perpendicular current, and j_ϕ^{RF} is the noninductive rf-driven current to render the central safety factor q_0 smaller than unity.